

Brain Tumor Segmentation Using Ensemble CNN-Transfer Learning Models: DeepLabV3plus and ResNet50 Approach

Shoffan Saifullah^{1,2}[0000–0001–6799–3834] and Rafal
Dreżewski¹[0000–0001–8607–3478]

¹ Faculty of Computer Science, AGH University of Krakow, Krakow 30-059, Poland
{saifulla,drezew}@agh.edu.pl

² Department of Informatics, Universitas Pembangunan Nasional Veteran
Yogyakarta, Yogyakarta 55281, Indonesia
shoffans@upnyk.ac.id

Abstract. This study investigates the impact of advanced computational methodologies on brain tumor segmentation in medical imaging, addressing challenges like interobserver variability and biases. The DeepLabV3plus model with ResNet50 integration is rigorously examined and augmented by diverse image enhancement techniques. The hybrid CLAHE-HE approach achieves exceptional efficacy with an accuracy of 0.9993, a Dice coefficient of 0.9690, and a Jaccard index of 0.9404. Comparative analyses against established models, including SA-GA, Edge U-Net, LinkNet, MAG-Net, SegNet, and Multi-class CNN, consistently demonstrate the proposed method’s robustness. The study underscores the critical need for continuous research and development to tackle inherent challenges in brain tumor segmentation, ensuring insights translate into practical applications for optimized patient care. These findings offer substantial value to the medical imaging community, emphasizing the indispensability of advancements in brain tumor segmentation methodologies. The study outlines a path for future exploration, endorsing ensemble models like U-Net, ResNet-U-Net, VGG-U-Net, and others to propel the field toward unprecedented frontiers in brain tumor segmentation research.

Keywords: Brain Tumor Segmentation · Deep Learning · Image enhancement · Medical Imaging · Ensemble Methods.

1 Introduction

Medical imaging, especially in brain tumor segmentation, has evolved significantly with the seamless integration of computational methods into neurology [1]. Despite the improved visualization of Magnetic Resonance Imaging (MRI), the complex nature of brain tumors necessitates advanced automated approaches [22]. Traditional manual segmentation introduces variability and biases, emphasizing the need for precise medical decisions in treatment planning, monitoring, and evaluating efficacy [9].

The rise of computational techniques, especially Convolutional Neural Networks (CNNs), has opened avenues to overcome manual brain tumor segmentation limitations [12]. Proficient in capturing intricate patterns, CNNs excel in delineating tumor regions [25]. However, challenges like data heterogeneity, class imbalance, and model generalization demand a shift to data-driven approaches [19]. Promising solutions like SegNet [30], LinkNet [39, 40], and U-Net [38, 3] with transfer learning [17, 32] require rigorous validation and robust data augmentation. While ResNet50 and U-Net perform well, addressing brain tumor imaging complexity necessitates efficient methods [3]. Correlating segmentation with patient survival emphasizes the need for accurate methods. Researchers advocate for comprehensive CNNs, demonstrating effectiveness in automated detection and proposing robust CNN U-Net models for medical-grade applications.

The motivation for this research arises from the imperative to overcome limitations in traditional manual brain tumor segmentation. Integrating computational techniques, particularly deep-learning models, offers a transformative opportunity to expedite analyses and produce highly accurate and reproducible results. This research aims to explore the effectiveness of CNN-Transfer Learning models [35, 37], proposing a novel approach that integrates DeepLabV3plus and ResNet50 for efficient and accurate brain tumor segmentation. Rigorous evaluation will compare the performance of this model against established benchmarks such as modified U-Net, SegNet, LinkNet, and others. Additionally, the research assesses the impact of image enhancement techniques, including a hybrid of Contrast-Limited Adaptive Histogram Equalization (CLAHE) and Histogram Equalization (HE), on segmentation accuracy [34, 33]. This multifaceted approach aims to advance our understanding of computational methods in medical imaging and contribute insights that may enhance the precision and efficiency of brain tumor segmentation.

The structure of this paper includes the following sections: Section 2 offers an overview of related works, emphasizing strengths and limitations. Section 3 details proposed methods addressing identified challenges, including DeepLabV3plus and ResNet50. Section 4 presents results, compares performance, and discusses implications. Finally, Section 5 concludes with a summary of contributions and potential avenues for future research in brain tumor segmentation.

2 Related Works

Research on brain tumor segmentation and ensemble CNN models has proven them to be effective in various medical imaging applications [23]. Studies on glioblastoma segmentation and ensemble learning in hyperspectral image processing [20] demonstrate their versatility. The ViT-CNN ensemble model excels in classifying acute lymphoblastic leukemia [11], emphasizing its potential in medical diagnosis.

Significant strides have been achieved in brain tumor segmentation, deep learning, and medical image analysis. The BRATS benchmark [28] has been

pivotal in unveiling computational challenges. Ensemble CNN models exhibit remarkable performance [5], emphasizing deep learning’s prowess in categorizing brain cancers. The importance of data augmentation [15], advancements like the U-Net application [13, 17, 3], and innovations such as dockerized segmentation algorithms contribute to the expanding research landscape. Refinements in U-Net architecture [21] and a novel patch-based dictionary learning algorithm extend segmentation methodologies. Contributions span from automatic segmentation methods to developing deep learning CNN models for segmentation and classification [9].

Further advances in brain tumor detection, such as the TransConver network, showcased the potential of transformer and convolution parallel networks [18]. High accuracy, particularly on the BraTS 2018 dataset, underscores the importance of dataset-specific evaluations [26]. Employing CNN, deep learning, and AI algorithms achieves notable accuracies in categorizing and identifying brain tumors. Additional research focuses on classifying and segmenting tumors using pre-trained AlexNet, advancing transfer learning for brain tumor classification, and addressing challenges in automated tumor analysis [41]. Demonstrated effectiveness in transfer learning for brain tumor multi-classification highlights its applicability across diverse scenarios. Emphasizing the role of automated segmentation in enhancing research precision, speed, and reproducibility in medical imaging is also underscored [24].

This research stands out as state-of-the-art within this rich landscape, presenting a significant advancement in brain tumor segmentation using ensemble CNN-Transfer Learning Models [35], specifically the DeepLabV3plus and ResNet50 approach. The proposed method not only leverages the strengths observed in previous studies but also addresses limitations, contributing to the continual refinement and progress in medical image analysis.

3 Materials and Methods

3.1 Brain MRI Datasets and Preprocessing

In this study, a comprehensive dataset comprising 3064 T1-CE MRIs obtained from 233 patients forms the foundation of our research [6]. The dataset is meticulously categorized into three distinct classes: meningiomas (708 images), gliomas (1426 images), and pituitary tumors (930 images). Each image within the dataset possesses a corresponding ground truth, represented by masks, enabling the identification of abnormal regions. Fig. 1 illustrates representative samples of brain MRI images accompanied by their respective ground truth masks, showcasing instances of Meningioma (a), Glioma (b), and Pituitary tumors (c).

To optimize the deep learning model’s processing efficiency, a crucial preprocessing step involves resizing the images to a standardized resolution of 256×256 pixels [34, 33]. This resizing facilitates computational efficiency and ensures consistency across diverse input images. Following the resizing process, image enhancement techniques are employed to elevate the overall quality of the images.

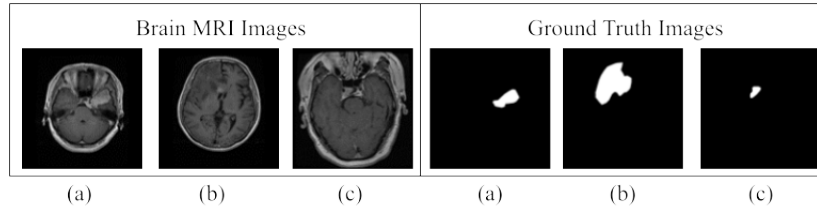


Fig. 1: Samples of brain MRI with the ground truth (masks) of (a) Meningioma, (b) Glioma, and (c) Pituitary.

The first scenario involves the application of Histogram Equalization (HE), a method widely recognized for enhancing image contrast. The second scenario employs Contrast Limited Adaptive Histogram Equalization (CLAHE) [34], which adapts the enhancement process to local regions, enhancing details in specific areas. The third and fourth scenarios involve hybrid approaches, combining HE and CLAHE in different sequences: HE-CLAHE and CLAHE-HE [34, 36]. These variations exploit the synergistic effects of global and local contrast enhancements. HE operates by redistributing the intensity levels of the image histogram to cover the entire available range. The transformation function $T(rk)$ (Eq. (1)) for each pixel intensity rk in the original image is calculated based on the image histogram $H(i)$, probability pixels $P_x(i)$, and commutative distribution function $cdf_x(i)$.

$$T(rk) = (L - 1) \cdot cdf_x(rk) \quad (1)$$

where L is the number of intensity levels. The commutative distribution function is computed by the sum of probabilities up to the intensity level rk (Eq. (2)).

$$cdf_x(rk) = \sum_{j=0}^{rk} P_x(j) \quad (2)$$

Finally, the probability pixels $P_x(j)$ are calculated as the ratio of pixels with intensity $H(i)$ to the total number of pixels (Eq. (3)).

$$P_x(j) = \frac{H(i)}{N} \quad (3)$$

where N is the total number of pixels. This process yields the distribution of the HE-transformed image $h(v)$, effectively enhancing contrast (Eq. (4)).

$$h(v) = \frac{cdf(v) - cdf_{min}}{n - cdf_{min}} \quad (4)$$

Unlike HE, CLAHE adapts its enhancement process with a clip limit (β), preventing over-enhancement and artifacts. The transformation function $T(rk)$ for each pixel intensity rk is given by Eq. (5). The clip limit β (Eq. (6)) controls the amount of contrast enhancement.

$$T(rk) = (L - 1) \frac{cdf_x(rk)}{\max(\beta - cdf_x(rk))} \quad (5)$$

$$\beta = \frac{M}{n} \left(1 + \frac{\alpha}{100} (S_{max} - 1) \right) \quad (6)$$

3.2 CNN-Transfer Learning Approaches: DeepLabV3plus with ResNet50

Our proposed approach utilizes ensemble CNN-Transfer Learning for brain tumor segmentation, integrating the DeepLabV3plus model [31] with the ResNet50 backbone [27], as illustrated in Fig. 2. This ensemble design allows for enhanced predictive capabilities, utilizing the strengths of both models to improve segmentation accuracy and generalization. We adopted a standard data split of 80% for training and 20% for validation, training the model with a learning rate of 10^{-3} and the Adam optimizer over 50 epochs, with a mini-batch size of 32 iterations. The combined architecture optimally captures contextual information and deep feature extraction, resulting in superior segmentation accuracy.

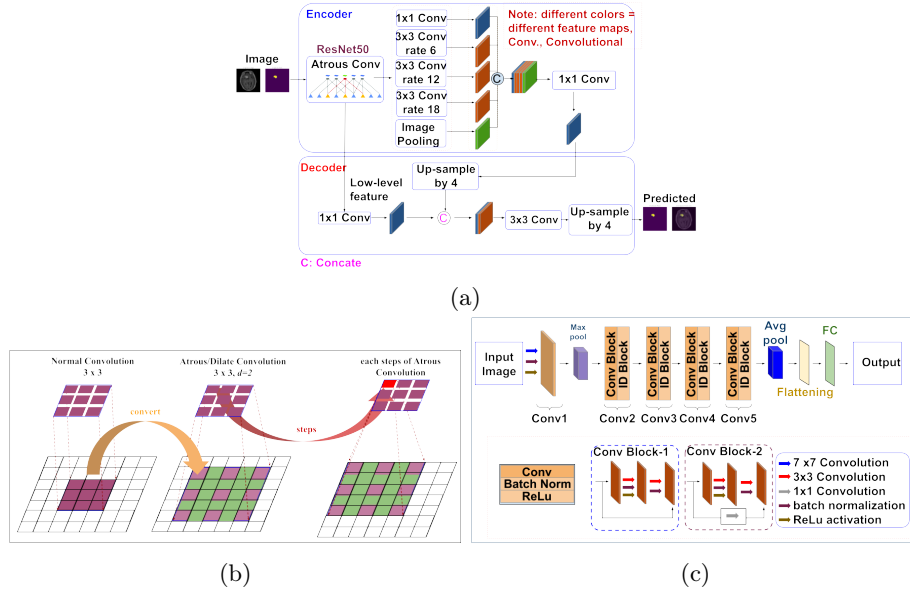


Fig. 2: Ensemble CNN-Transfer Learning Architecture: (a) DeepLabV3plus model, (b) the transformation from standard convolution to Atrous/Dilated convolution showcasing sequential processing of dilation pixels, (c) ResNet50 backbone utilized for accurate prediction in brain tumor segmentation.

DeepLabv3plus Layers are architectural innovations which play a central role in the proficiency of our ensemble CNN-transfer learning system for brain tumor prediction and segmentation (Fig. 2(a)). DeepLabv3plus brings advanced semantic segmentation capabilities to the model, explicitly emphasizing the precise delineation of object boundaries, a critical requirement in medical image analysis [2]. The architecture includes atrous convolution, also known as dilated convolution, which allows for an expanded receptive field without an increase in model parameters. This feature enables the accurate segmentation of brain tumors by capturing information from fine-grained to high-level features.

Atrous Spatial Pyramid Pooling (ASPP) is another essential element that utilizes parallel dilated convolutions to capture multiscale information effectively, ensuring recognition of both large and small tumor regions (Fig. 2(b)). Additionally, feature refinement and decoder modules contribute to model precision, allowing the distinction of tumor boundaries even in complex images. These layers significantly enhance the model’s proficiency in brain tumor segmentation.

Further enhancing the understanding of Atrous Convolution, Fig. 2(b) illustrates the transformation from standard convolution to Atrous/Dilated convolution. The first two diagrams in Fig. 2(b) depict the fundamental shift in the convolutional operation, highlighting how Atrous convolution introduces gaps in the filter, enabling the model to capture information from a broader context. The third diagram in Fig. 2(b) illustrates the sequential processing of dilation pixels, emphasizing the stepwise integration of contextual information. This mechanism is pivotal in our approach, as it empowers the model to better discern fine details and boundaries in brain tumor images.

Fig. 2(c) delves into the ResNet50 architecture, particularly emphasizing the Atrous Convolutional layer. This layer plays a crucial role in feature extraction, allowing the model to capture intricate spatial dependencies within brain tumor images. The utilization of Atrous Convolution enhances the network’s receptive field, enabling the extraction of more contextual information for improved segmentation performance.

3.3 Performance Evaluation Metrics for Segmentation Approach

The evaluation of our segmentation approach relies on key performance metrics [35], each providing valuable insights into the model’s effectiveness [16]. Accuracy (ACC) is the fundamental metric that quantifies the overall correctness of the model’s predictions by considering true positives (TP), true negatives (TN), false positives (FP), and false negatives (FN). The accuracy computes the ratio of correctly classified pixels to the total number of pixels (Eq. (7)).

$$ACC = \frac{(TP + TN)}{(TP + TN + FP + FN)} \quad (7)$$

The loss function (L) serves as a measure of dissimilarity between predicted and ground truth masks. Often expressed as cross-entropy, the loss is calculated by Eq. (8), where y represents the ground truth, \hat{y} is the predicted mask, and N is the total number of pixels.

$$L(y, \hat{y}) = -\frac{1}{N} \sum_{i=1}^N yi \cdot \log(\hat{y}i) + (1 - yi) \cdot \log(1 - \hat{y}i) \quad (8)$$

The Dice coefficient, denoted as Dice, assesses spatial overlap and is computed by Eq. (9). A higher Dice coefficient indicates better spatial alignment between the predicted and ground truth tumor regions.

$$Dice = \frac{(2xTP)}{(2xTP + FP + FN)} \quad (9)$$

The Jaccard index, or Intersection over Union (IoU), measures region similarity and is given by Eq. (10). This metric considers the common area between the predicted and actual tumor regions.

$$Jaccard = \frac{(TP)}{(TP + FP + FN)} \quad (10)$$

4 Results and Discussion

In this section, we present the results of our proposed approach, which integrates DeepLabV3plus and ResNet50 for brain tumor segmentation. Our model is evaluated using the BRATS dataset [6], and we compare its performance with established benchmarks from other researchers. Additionally, we explore the impact of image enhancement techniques, such as HE, CLAHE, and hybrid approaches, on segmentation accuracy.

4.1 Results of CNN-Transfer Learning for Brain Tumor Segmentation: DeepLabV3plus and ResNet50 Approach

This section presents an in-depth exploration of the DeepLabV3plus model with the ResNet50 backbone for brain tumor segmentation. It sheds light on the nuanced impact of various image enhancement strategies on its performance. Four pivotal performance metrics—accuracy, loss, Dice, and Jaccard indices—are meticulously employed to provide a holistic understanding of the model’s proficiency across diverse preprocessing techniques. The evaluated model variants encompass image enhancement methods, including HE, CLAHE, and hybrid approaches (HE-CLAHE and CLAHE-HE), as summarized in Table 1.

Commencing with the baseline scenario without image enhancement (“-”), the model achieves an impressive accuracy of 0.9987. However, the discerning analysis of the Dice coefficient (0.9409) and Jaccard index (0.9048) unveils potential areas for improvement, specifically in capturing the intricate boundaries of brain tumors. Subsequent exploration of image enhancement strategies reveals HE as a pivotal technique, showcasing notable improvements. HE yields the accuracy of 0.9991, reduced loss (0.0020), and significant advancements in Dice (0.9618) and Jaccard (0.9270) indices, underlining its efficacy in contrast enhancement

Table 1: Comparison of brain tumor segmentation performance using different image enhancement techniques.

Image Enhancement	DeepLabV3plus with ResNet50		
	Accuracy	Loss	Dice Jaccard
-	0.9987	0.0031	0.9409 0.9048
HE	0.9991	0.0020	0.9618 0.9270
CLAHE	0.9990	0.0024	0.9558 0.9160
HE-CLAHE	0.9991	0.0021	0.9599 0.9242
CLAHE-HE	0.9993	0.0019	0.9690 0.9404

for more precise tumor region segmentation. Building upon the success of HE, CLAHE contributes to further refinement, achieving the accuracy of 0.9990 and showcasing benefits in capturing local details, particularly in enhancing local features within brain tumor imaging data.

The combination of HE and CLAHE (HE-CLAHE) exhibits a synergistic effect, yielding an accuracy of 0.9991 and higher Dice (0.9599) and Jaccard (0.9242) indices. This combination underscores the importance of a judicious blend of global and local contrast enhancements for superior segmentation outcomes, with the sample of results in Fig. 3.

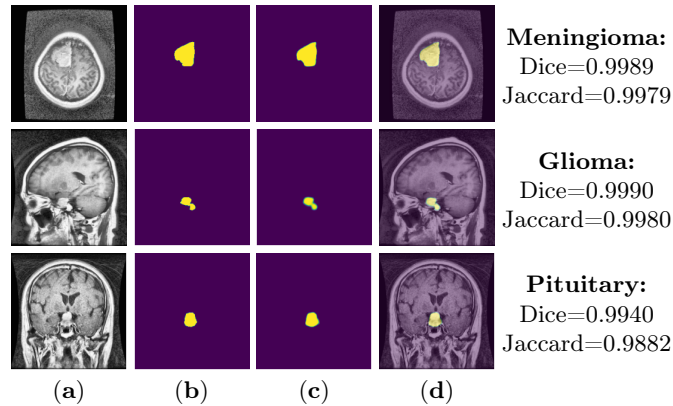


Fig. 3: Sample of segmentation results illustrating (a) brain MRI with CLAHE-HE, (b) ground truth (mask), (c) predictions from our proposed method, and (d) overlap of the original image.

Notably, reversing the order of enhancement techniques (CLAHE-HE) yields the highest overall performance, emphasizing the significance of the sequence in optimizing the model's ability to capture intricate details in brain tumor images. The results highlight that a careful consideration of preprocessing sequences tailored to the characteristics of medical imaging data significantly influences the model's segmentation efficacy. The model achieves its peak performance

with CLAHE-HE image enhancement, as confirmed by the graph evaluation in Fig. 4, demonstrating the robustness and stability of the proposed approach across diverse brain tumor segmentation scenarios.

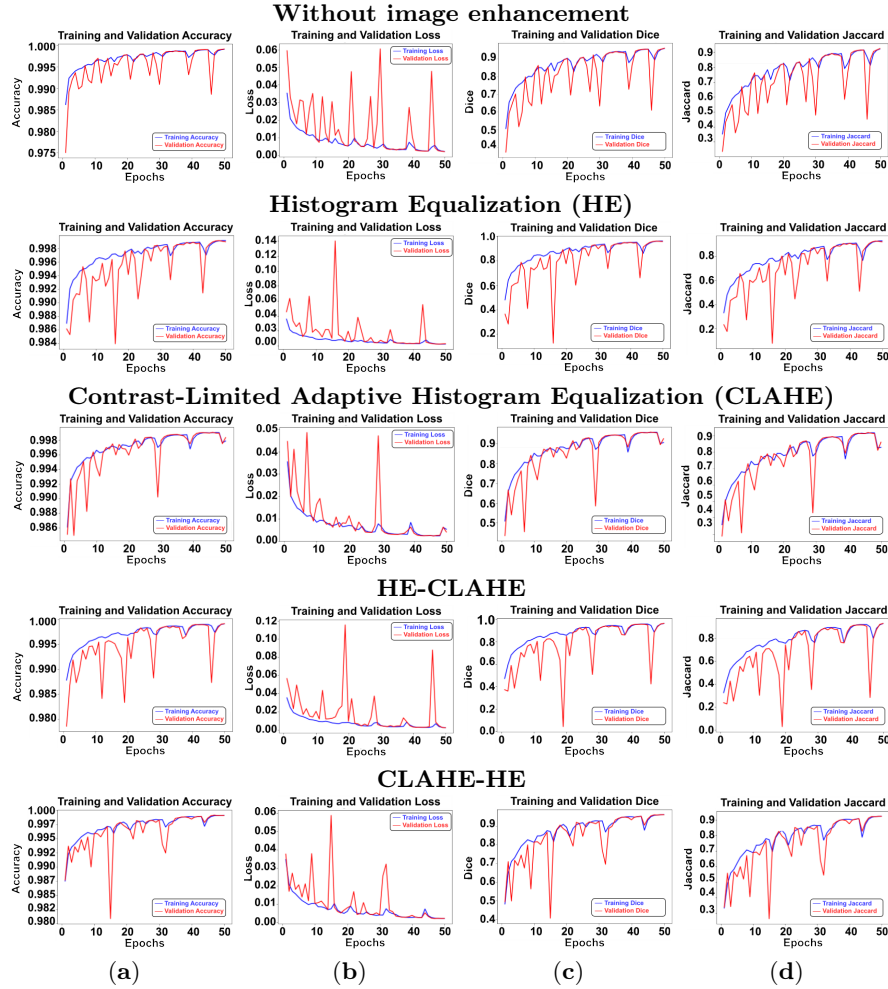


Fig. 4: Performance evaluation metrics of the proposed DeepLabV3plus with ResNet50 model based on (a) Accuracy, (b) Loss, (c) Dice, and (d) Jaccard indices, showcasing the impact of various image enhancement scenarios on brain tumor segmentation proficiency.

4.2 Comparison of the Proposed Method with Other Approaches

This section provides a nuanced analysis of our proposed method’s segmentation performance across specific brain tumor classes, including Meningioma, Glioma, and Pituitary, compared to previous studies, as shown in Table 2. The evaluation metrics considered are accuracy, Dice coefficient, and Jaccard index.

Table 2: Comparison of segmentation efficacy in individual classes of brain tumors for different methods.

Method	Dataset (Class)	Accuracy	Dice	Jaccard
Proposed Method		0.9995	0.9809	0.9627
SA-GA [14]	Meningioma	0.8777	-	-
Edge U-Net [21]		-	0.8880	0.7743
Multiclass CNN [7]		-	0.8940	-
Proposed Method		0.9995	0.9596	0.9233
SA-GA [14]	Glioma	0.9785	-	-
Edge U-Net [21]		-	0.9176	0.8747
Multiclass CNN [7]		-	0.7790	-
Proposed Method		0.9995	0.9600	0.9240
SA-GA [14]	Pituitary	0.9512	-	-
Edge U-Net [21]		-	0.8728	0.7985
Multiclass CNN [7]		-	0.8130	-

As detailed in Table 2, our proposed method demonstrates exceptional segmentation performance for Meningioma, achieving the remarkable accuracy of 0.9995. The Dice coefficient (0.9809) and Jaccard index (0.9627) further underscore the precision in delineating Meningioma boundaries. In contrast, the comparison with SA-GA, Edge U-Net, and Multi-class CNN reveals notable superiority, signifying the efficacy of our approach in capturing the intricate details of Meningioma structures. Our method outperforms existing models, showcasing its potential for accurate Meningioma segmentation in medical imaging.

In the case of Glioma, as illustrated in Table 2, our proposed method continues to excel with the accuracy of 0.9995, indicating robust segmentation capabilities. The Dice coefficient (0.9596) and Jaccard index (0.9233) further validate the accuracy and precision in capturing Glioma regions. Compared to SA-GA, Edge U-Net, and Multi-class CNN, our method consistently outperforms these models, emphasizing its effectiveness in Glioma segmentation. The superior performance underscores the potential clinical relevance of our method for accurate Glioma delineation in medical images.

As depicted in Table 2, our method achieves outstanding results in Pituitary segmentation, attaining the accuracy of 0.9995. The Dice coefficient (0.9600) and Jaccard index (0.9240) further highlight the efficacy of our approach in capturing Pituitary tumor structures. In contrast to SA-GA, Edge U-Net, and Multi-class CNN, our method demonstrates superior segmentation performance. The results affirm the applicability of our proposed method for precise Pituitary tumor segmentation, showcasing its potential impact on diagnostic accuracy.

The overall comparison across different brain tumor classes emphasizes the versatility and consistency of our proposed method. By outperforming existing models across multiple tumor types, our method showcases its robustness and potential applicability in diverse clinical scenarios. The superior segmentation outcomes across Meningioma, Glioma, and Pituitary tumors collectively contribute to the comprehensive effectiveness of our proposed method in brain tumor segmentation.

4.3 Comparative Analysis of Segmentation Performance Across All Data

This section thoroughly analyzes our proposed method’s segmentation performance across diverse datasets, benchmarking it against various state-of-the-art models detailed in Table 3. Key evaluation metrics, including accuracy, Dice coefficient, and Jaccard index, offer a comprehensive understanding of the overall effectiveness of our approach. The results in Table 3 underscore the robust performance of our method, boasting an impressive accuracy of 0.9993, with a high Dice coefficient (0.9690) and Jaccard index (0.9404), validating its efficacy in precisely delineating brain tumor structures. This overall excellence highlights the versatility of our approach, positioning it as a compelling choice for diverse medical imaging applications.

Table 3: Comparison of segmentation efficacy across all data with different approaches.

Method	Accuracy	Dice	Jaccard
Proposed Method	0.9993	0.9690	0.9404
DeepLabV3plus ResNet18 [35]	0.9124	0.9340	0.9748
SegNet CNN-Autoencoder [4]	0.9917	0.7287	-
SA-GA [14]	0.9590	-	-
SegNet [30]	0.9340	0.9314	-
U-Net with ResNet [17]	0.9960	0.9011	-
U-Net [13]	0.9780	0.7800	-
Multiclass CNN [7]	-	0.8280	-
MAG-Net [8]	0.9952	0.7400	0.6000
Hybrid KFCM-CNN [29]	0.9760	0.8884	0.8204
U-Net based [3]	-	0.8900	0.8100
Cascaded Dual-Scale LinkNet [39]	-	0.8003	0.9074
SegNet-VGG-16 [30]	0.9340	0.9314	0.914
2D-UNet [38]	92.1600	0.8120	-
CNN with LinkNet [40]	-	0.7300	-
U-Net with adaptive thresholding [10]	0.9907	0.6239	-
O2U-Net [42]	0.9934	0.8083	-
CNN U-Net [32]	0.9854	-	0.8196

Our proposed method consistently exhibits superior performance across all metrics compared to a range of existing models. Outperforming DeepLabV3plus ResNet18, SegNet CNN-Autoencoder, and others, our method showcases advancements in segmentation quality, achieving higher accuracy and excelling in

both Dice and Jaccard metrics. These results underscore its effectiveness in capturing intricate details, emphasizing its potential for accurate and reliable brain tumor segmentation. Moreover, the method surpasses modified U-Net, SegNet, and LinkNet in accuracy, Dice, and Jaccard metrics, reinforcing its efficacy across a diverse range of existing models and highlighting its potential for widespread adoption in clinical and research settings.

5 Conclusion

In conclusion, our study presents a pioneering approach to brain tumor segmentation, leveraging the DeepLabV3plus model with ResNet50 and incorporating diverse image enhancement techniques. We have identified the sequence-dependent impact of enhancement methods through meticulous analysis, highlighting the superior performance of the hybrid CLAHE-HE approach. Our model demonstrated exceptional proficiency in segmenting diverse brain tumor classes, achieving outstanding metrics with an accuracy of 0.9993, a Dice coefficient of 0.9690, and a Jaccard index of 0.9404, surpassing existing methods. The robustness of our proposed method across all data further underscores its effectiveness compared to state-of-the-art models.

While providing valuable insights for medical image analysis, this study acknowledges potential limitations and emphasizes the imperative need for future research to enhance generalizability and address variations in imaging protocols. As part of our future work, exploring ensemble models by integrating our proposed method with architectures such as modified U-Net, ResNet-U-Net, VGG-U-Net, and others could further elevate segmentation performance, contributing to the evolution of advanced medical imaging techniques.

Acknowledgement. This research was supported by the Polish Ministry of Science and Higher Education funds assigned to AGH University of Krakow and by PLGrid under grant no. PLG/2023/016757.

References

1. Ahamed, M.F., Hossain, M.M., Nahiduzzaman, M., Islam, M.R., Islam, M.R., Ahsan, M., Haider, J.: A review on brain tumor segmentation based on deep learning methods with federated learning techniques. *Computerized Medical Imaging and Graphics* **110**, 102313 (2023). <https://doi.org/10.1016/j.compmedimag.2023.102313>
2. Akcay, O., Kinaci, A.C., Avsar, E.O., Aydar, U.: Semantic Segmentation of High-Resolution Airborne Images with Dual-Stream DeepLabV3+. *ISPRS International Journal of Geo-Information* **11**(1), 23 (2021). <https://doi.org/10.3390/ijgi11010023>
3. Akter, A., Nosheen, N., Ahmed, S., Hossain, M., Yousuf, M.A., Almoayad, M.A.A., Hasan, K.F., Moni, M.A.: Robust clinical applicable CNN and U-Net based algorithm for MRI classification and segmentation for brain tumor. *Expert Systems with Applications* **238**, 122347 (2024). <https://doi.org/10.1016/j.eswa.2023.122347>

4. Badža, M.M., Barjaktarović, M.Č.: Segmentation of Brain Tumors from MRI Images Using Convolutional Autoencoder. *Applied Sciences* **11**(9), 4317 (2021). <https://doi.org/10.3390/app11094317>
5. Beliveau, V., Nørgaard, M., Birkl, C., Seppi, K., Scherfler, C.: Automated segmentation of deep brain nuclei using convolutional neural networks and susceptibility weighted imaging. *Human Brain Mapping* **42**(15), 4809–4822 (2021). <https://doi.org/10.1002/hbm.25604>
6. Cheng, J., Huang, W., Cao, S., Yang, R., Yang, W., Yun, Z., Wang, Z., Feng, Q.: Enhanced Performance of Brain Tumor Classification via Tumor Region Augmentation and Partition. *PLOS ONE* **10**(10), e0140381 (2015). <https://doi.org/10.1371/journal.pone.0140381>
7. Díaz-Pernas, F.J., Martínez-Zarzuela, M., Antón-Rodríguez, M., González-Ortega, D.: A Deep Learning Approach for Brain Tumor Classification and Segmentation Using a Multiscale Convolutional Neural Network. *Healthcare* **9**(2), 153 (2021). <https://doi.org/10.3390/healthcare9020153>
8. Gupta, S., Pun, N.S., Sonbhadra, S.K., Agarwal, S.: MAG-Net: Multi-task Attention Guided Network for Brain Tumor Segmentation and Classification. In: Srirama, S.N., Lin, J.C.W., Bhatnagar, R., Agarwal, S., Reddy, P.K. (eds) *Big Data Analytics. BDA 2021. Lecture Notes in Computer Science* **13147**, 3–15 (2021). https://doi.org/10.1007/978-3-030-93620-4_1
9. Hoebel, K.V., Bridge, C.P., Kim, A., Gerstner, E.R., Ly, I.K., Deng, F., DeSalvo, M.N., Diettrich, J., Huang, R., Huang, S.Y., Pomerantz, S.R., Vagvala, S., Rosen, B.R., Kalpathy-Cramer, J.: Not without Context—A Multiple Methods Study on Evaluation and Correction of Automated Brain Tumor Segmentations by Experts. *Academic Radiology* (2023). <https://doi.org/10.1016/j.acra.2023.10.019>
10. Isunuri, B.V., Kakarla, J.: Fast brain tumour segmentation using optimized U-Net and adaptive thresholding. *Automatika* **61**(3), 352–360 (2020). <https://doi.org/10.1080/00051144.2020.1760590>
11. Jiang, Z., Dong, Z., Wang, L., Jiang, W.: Method for Diagnosis of Acute Lymphoblastic Leukemia Based on ViT-CNN Ensemble Model. *Computational Intelligence and Neuroscience* **2021**, 1–12 (2021). <https://doi.org/10.1155/2021/7529893>
12. Jyothi, P., Singh, A.R.: Deep learning models and traditional automated techniques for brain tumor segmentation in MRI: a review. *Artificial Intelligence Review* **56**(4), 2923–2969 (2023). <https://doi.org/10.1007/s10462-022-10245-x>
13. Kasar, P.E., Jadhav, S.M., Kansal, V.: MRI Modality-based Brain Tumor Segmentation Using Deep Neural Networks. *Research Square* (2021). <https://doi.org/10.21203/rs.3.rs-496162/v1>
14. Kharrat, A., Neji, M.: Feature selection based on hybrid optimization for magnetic resonance imaging brain tumor classification and segmentation. *Applied Medical Informatics* **41**(1), 9–23 (2019)
15. Kulkarni, S.M., Sundari, G.: Brain MRI Classification using Deep Learning Algorithm. *International Journal of Engineering and Advanced Technology* **9**(3), 1226–1231 (2020). <https://doi.org/10.35940/ijeat.C5350.029320>
16. Kumar, A.: Study and analysis of different segmentation methods for brain tumor MRI application. *Multimedia Tools and Applications* **82**(5), 7117–7139 (2023). <https://doi.org/10.1007/s11042-022-13636-y>
17. Kumar Sahoo, A., Parida, P., Muralibabu, K., Dash, S.: Efficient simultaneous segmentation and classification of brain tumors from MRI scans using deep learning. *Biocybernetics and Biomedical Engineering* **43**(3), 616–633 (2023). <https://doi.org/10.1016/j.bbe.2023.08.003>

18. Liang, J., Yang, C., Zeng, M., Wang, X.: TransConver: transformer and convolution parallel network for developing automatic brain tumor segmentation in MRI images. *Quantitative Imaging in Medicine and Surgery* **12**(4), 2397–2415 (apr 2022). <https://doi.org/10.21037/qims-21-919>
19. Liu, X., Shih, H.A., Xing, F., Santarnecchi, E., El Fakhri, G., Woo, J.: Incremental Learning for Heterogeneous Structure Segmentation in Brain Tumor MRI. In: Greenspan, H., et al. *Medical Image Computing and Computer Assisted Intervention – MICCAI 2023*. MICCAI 2023. *Lecture Notes in Computer Science* **14221**, 46–56 (2023). https://doi.org/10.1007/978-3-031-43895-0_5
20. Lv, Q., Feng, W., Quan, Y., Dauphin, G., Gao, L., Xing, M.: Enhanced-Random-Feature-Subspace-Based Ensemble CNN for the Imbalanced Hyperspectral Image Classification. *IEEE Journal of Selected Topics in Applied Earth Observations and Remote Sensing* **14**, 3988–3999 (2021). <https://doi.org/10.1109/JSTARS.2021.3069013>
21. M. Gab Allah, A., M. Sarhan, A., M. Elshennawy, N.: Edge U-Net: Brain tumor segmentation using MRI based on deep U-Net model with boundary information. *Expert Systems with Applications* **213**, 118833 (2023). <https://doi.org/10.1016/j.eswa.2022.118833>
22. Metlek, S., Çetner, H.: ResUNet+: A New Convolutional and Attention Block-Based Approach for Brain Tumor Segmentation. *IEEE Access* **11**, 69884–69902 (2023). <https://doi.org/10.1109/ACCESS.2023.3294179>
23. Mouhafid, M., Salah, M., Yue, C., Xia, K.: Deep Ensemble Learning-Based Models for Diagnosis of COVID-19 from Chest CT Images. *Healthcare* **10**(1), 166 (2022). <https://doi.org/10.3390/healthcare10010166>
24. Najjar, R.: Redefining Radiology: A Review of Artificial Intelligence Integration in Medical Imaging. *Diagnostics* **13**(17), 2760 (2023). <https://doi.org/10.3390/diagnostics13172760>
25. Neamah, K., Mohamed, F., Adnan, M.M., Saba, T., Bahaj, S.A., Kadhim, K.A., Khan, A.R.: Brain Tumor Classification and Detection Based DL Models: A Systematic Review. *IEEE Access* pp. 1–1 (2023). <https://doi.org/10.1109/ACCESS.2023.3347545>
26. Nguyen, H.T.T., Pham, T.T.H., Le, H.T.: Application of deep learning in brain tumor segmentation. *Science & Technology Development Journal - Engineering and Technology* (2022). <https://doi.org/10.32508/stdjet.v5i2.951>
27. Polat, H.: Multi-task semantic segmentation of CT images for COVID-19 infections using DeepLabV3+ based on dilated residual network. *Physical and Engineering Sciences in Medicine* **45**(2), 443–455 (2022). <https://doi.org/10.1007/s13246-022-01110-w>
28. Ramasamy, G., Singh, T., Yuan, X.: Multi-Modal Semantic Segmentation Model using Encoder Based Link-Net Architecture for BraTS 2020 Challenge. *Procedia Computer Science* **218**, 732–740 (2023). <https://doi.org/10.1016/j.procs.2023.01.053>
29. Rao, S.K.V., Lingappa, B.: Image Analysis for MRI Based Brain Tumour Detection Using Hybrid Segmentation and Deep Learning Classification Technique. *International Journal of Intelligent Engineering and Systems* **12**(5), 53–62 (2019). <https://doi.org/10.22266/ijies2019.1031.06>
30. Rehman, A., Naz, S., Naseem, U., Razzak, I., Hameed, I.A.: Deep Autoencoder-Decoder Framework for Semantic Segmentation of Brain Tumor. *Aust. J. Intell. Inf. Process. Syst* **15**(4), 53–60 (2019)

31. Roy Choudhury, A., Vanguri, R., Jambawalikar, S.R., Kumar, P.: Segmentation of Brain Tumors Using DeepLabv3+. In: Crimi, A., Bakas, S., Kuijf, H., Keyvan, F., Reyes, M., van Walsum, T. (eds) *Brainlesion: Glioma, Multiple Sclerosis, Stroke and Traumatic Brain Injuries. BrainLes 2018. Lecture Notes in Computer Science* **11384**, 154–167 (2019). https://doi.org/10.1007/978-3-030-11726-9_14
32. Ruiz, C.B.: Classification and Segmentation of Brain Tumor MRI Images Using Convolutional Neural Networks. In: *2023 IEEE International Conference on Engineering Veracruz (ICEV)*. pp. 1–6. IEEE (2023). <https://doi.org/10.1109/ICEV59168.2023.10329651>
33. Saifullah, S., Dreżewski, R.: Enhanced Medical Image Segmentation using CNN based on Histogram Equalization. *2023 2nd International Conference on Applied Artificial Intelligence and Computing (ICAAIC)* pp. 121–126 (2023). <https://doi.org/10.1109/ICAAIC56838.2023.10141065>
34. Saifullah, S., Dreżewski, R.: Modified Histogram Equalization for Improved CNN Medical Image Segmentation. *Procedia Computer Science* **225**(C), 3021–3030 (2023). <https://doi.org/10.1016/j.procs.2023.10.295>
35. Saifullah, S., Dreżewski, R.: Redefining brain tumor segmentation: a cutting-edge convolutional neural networks-transfer learning approach. *International Journal of Electrical and Computer Engineering (IJECE)* **14**(3), 2583 (jun 2024). <https://doi.org/10.11591/ijece.v14i3.pp2583-2591>
36. Saifullah, S., Suryotomo, A.P.: Thresholding and Hybrid CLAHE-HE for Chicken Egg Embryo Segmentation. *2021 International Conference on Communication & Information Technology (ICICT)* pp. 268–273 (jun 2021). <https://doi.org/10.1109/ICICT52195.2021.9568444>
37. Saifullah, S., Suryotomo, A.P., Dreżewski, R., Tanone, R., Tundo: Optimizing Brain Tumor Segmentation Through CNN U-Net with CLAHE-HE Image Enhancement. *Proceedings of the 2023 1st International Conference on Advanced Informatics and Intelligent Information Systems (ICAI3S 2023)* pp. 90–101 (2024). https://doi.org/10.2991/978-94-6463-366-5_9
38. Sailunaz, K., Bestepe, D., Alhaji, S., Özyer, T., Rokne, J., Alhaji, R.: Brain tumor detection and segmentation: Interactive framework with a visual interface and feedback facility for dynamically improved accuracy and trust. *PLOS ONE* **18**(4), e0284418 (2023). <https://doi.org/10.1371/journal.pone.0284418>
39. Sobhaninia, Z., Rezaei, S., Karimi, N., Emami, A., Samavi, S.: Brain Tumor Segmentation by Cascaded Deep Neural Networks Using Multiple Image Scales. In: *2020 28th Iranian Conference on Electrical Engineering (ICEE)*. pp. 1–4. IEEE (2020). <https://doi.org/10.1109/ICEE50131.2020.9260876>
40. Sobhaninia, Z., Rezaei, S., Noroozi, A., Ahmadi, M., Zarrabi, H., Karimi, N., Emami, A., Samavi, S.: Brain Tumor Segmentation Using Deep Learning by Type Specific Sorting of Images (2018), <http://arxiv.org/abs/1809.07786>
41. Wahlang, I., Maji, A.K., Saha, G., Chakrabarti, P., Jasinski, M., Leonowicz, Z., Jasinska, E.: Brain Magnetic Resonance Imaging Classification Using Deep Learning Architectures with Gender and Age. *Sensors* **22**(5), 1766 (2022). <https://doi.org/10.3390/s22051766>
42. Zargari, S.A., Kia, Z.S., Nickfarjam, A.M., Hieber, D., Holl, F.: Brain Tumor Classification and Segmentation Using Dual-Outputs for U-Net Architecture: O2U-Net. *Studies in Health Technology and Informatics* **305**, 93–96 (2023). <https://doi.org/10.3233/SHTI230432>